Microsecond Laser Polarimetry for Emissivity Measurements on Liquid Metals at High Temperatures—Application to Niobium[1]

A. Seifter,[2] **F. Sachsenhofer,**[2] **S. Krishnan,**[3] **and G. Pottlacher**[2, 4]

Prior to now, all existing pulse heating systems capable of investigations on liquid samples could measure the radiance temperature only during the experiment. To determine the true temperature, it was necessary to assume that the emissivity is constant over the entire temperature range, with a value equal to that at the melting point. This assumption can cause large uncertainties in temperature measurements, especially at elevated temperatures. To avoid these uncertainties, a microsecond-division of amplitude photopolarimeter (μs-DOAP) was added to our experiment. The μs-DOAP detects changes in the polarization state of a laser beam ($\lambda = 684.5$ nm) reflected by the sample surface during the pulse-heating experiments. This change in the polarization state is used to determine the index of refraction n and the extinction coefficient, k. This leads to the reflectivity R of the sample, and by means of Kirchhoff's law for opaque materials, the normal spectral emissivity is obtained. The application of simultaneous laser polarimetry and spectral radiometry leads to the true temperature and is demonstrated on liquid niobium.

KEY WORDS: laser polarimetry; liquid metals; niobium; normal spectral emissivity.

1. INTRODUCTION

Thermophysical data such as enthalpy, specific heat capacity, thermal conductivity, thermal diffusivity, and specific electrical resistivity have been

measured for about 15 years at the Institut für Experimentalphysik in Graz by using fast pulse-heating techniques [1–3]. Among the properties of most interest is the absolute specimen temperature. Due to the high temperatures achieved and the short duration of the experiment, the temperature measurement must be performed by optical methods. This requires the use of fast pyrometers and knowledge about the behavior of the normal spectral emissivity as a function of temperature. Normal spectral emissivity measurements in the solid state employ two well-proven methods. In the case of the so-called blackbody technique, a small hole is machined into the sample. If the ratio of the depth of this hole to the diameter is higher than 10, this hole behaves like a blackbody source [4]; i.e., if one measures the radiation intensity emitted by this hole with a calibrated pyrometer, the true temperature can be determined. If the radiance temperature is also measured at the sample surface (if possible, near the blackbody hole, to avoid uncertainties due to temperature gradients), one obtains the normal spectral emissivity at the wavelength of the pyrometer from the ratio of the two intensities with the aid of Planck's radiation law.

Another method to determine emissivity in the solid state is the integrating sphere technique [5]. An integrating sphere is positioned close to the surface of the sample (a strip in this case). The sample surface is illuminated with a modulated laser beam, and the reflected intensity is collected in the sphere and detected with a photodiode. By means of a lock-in technique, to eliminate the background radiation of the hot sample, a signal proportional to the spectral hemispherical reflectivity of the sample is measured. Comparisons to a $BaSO_4$ reference mounted in the sphere provides the absolute value of reflectance of the sample, and the normal spectral emissivity of the specimen is obtained with the aid of Kirchoff's law. However, these two methods are applicable only to the solid state, since, on the one hand, the blackbody source would collapse due to surface tension in the liquid phase and, on the other hand, evaporation from the liquid metal would coat and destroy the inner surface of the integrating sphere.

A method of measurement which is applicable to both the solid and the liquid states is laser polarimetry [6]. With conventional polarimeters the reflected laser beam is often analyzed by means of a rotating polarizer and/or retarder and Fourier analysis of the transmitted signal. These devices are not suitable for use in rapid pulse-heating experiments.

Recently, polarimeters with no moving parts have been developed [4]. The microsecond-division of amplitude photopolarimeter (μs-DOAP) is one such device in which the light reflected from the sample is divided into two phase-shifted beams by means of a coated beam splitter, and each of these two beams is again divided by a Glan–Thomson polarizing prism, to

yield four light fluxes. With a suitable optical design, the polarization states of the four partial beams are independent and the four components of the Stokes vector $\mathbf{S} = (S_0, S_1, S_2, S_3)$ can be calculated from the four measured intensities $\mathbf{I} = (I_0, I_1, I_2, I_3)$ using a 4×4 array that represents the instrument matrix, $\mathbf{F}$, of the DOAP.

Once the Stokes parameters of the reflected light are measured, the normal spectral emissivity (at the wavelength of the laser; in the present case, 684.5 nm) can be calculated from the change in the polarization state of the reflected laser beam as described in the following sections.

2. MEASUREMENTS

2.1. Temperature

The optics of the pyrometer views an area of 0.2×10 mm of the sample surface at a 1:1 magnification onto the rectangular entry slit of an optical waveguide. The interference filter with a center wavelength of 650 nm and a half-power bandwidth of 37 nm is in front of the entry slit of the waveguide. The light delivered by this waveguide is detected by a Si photodiode and amplified with a fast amplifier (bandwidth of 1 MHz). The intensity signal J can be expressed as

$$J(\lambda, T) = g\sigma(\lambda)\,\tau(\lambda)\,\varepsilon_\lambda(\lambda, T)\,\frac{c_1}{\lambda^5[e^{\frac{c_2}{\lambda \cdot T}} - 1]} \tag{1}$$

where g is the geometry factor; σ, the sensitivity of the electronics and diode; λ, the wavelength; τ, the transmission of the optics and optical waveguide; ε_λ, the normal spectral emissivity; c_1 and c_2, the first and second radiation constants; and T, the temperature.

For a calibrated pyrometer the following relation between the detected intensity signal and the radiance temperature is valid:

$$T_{\mathrm{Rad}} = \frac{c_2}{\lambda \ln((K/J) + 1)} \tag{2}$$

where K is the calibration factor and J is the pyrometer signal.

Equation (2) is valid only for very narrow-bandwidth instruments, in which the pyrometer effective wavelength does not change significantly in the temperature range. For a bandwidth of 37 nm in the temperature range 1500 to 3000 K, we calculated the mean effective wavelength dependence

on the temperature (assuming a Gaussianfilter curve and a linear dependence of the wavelength of the detector response) of ± 2 nm in this temperature range. The temperature error caused by assuming a constant wavelength over this temperature interval is less than ± 3 K. For the tungsten filament lamp that is used for calibration, a temperature uncertainty of ± 7 K is given; thus, the use of a constant wavelength for temperature evaluation is rectified.

The unknown quantities g, σ, and τ are combined into the calibration factor K, which requires only a linear amplifier and is independent of temperature. From Planck's radiation law the relation between radiance temperature and true temperature is given by

$$T_{\text{true}} = \frac{c_2}{\lambda} \frac{1}{\ln\left[\varepsilon\left(e^{\frac{c_2}{\lambda \cdot T_{\text{Rad}}}} - 1\right) + 1\right]} \tag{3}$$

To keep the laser light (684.5 nm, used for polarimetry) out of the pyrometer, the center wavelength of the pyrometer was set at 650 nm (bandwidth of 37 nm), as 650 nm is one of the standard wavelengths of pyrometry. The difference between the emissivity measurements at 684.5 nm and the temperature measurements at 650 nm will cause a temperature uncertainty of not more than 3 K at melting, increasing to 6 K at 3500 K. Furthermore, the linearity of the pyrometer used was proven by different intensities of the tungsten filament lamp and the variation of the K factor was negligible.

Prior to this work, all experiments involving rapid pulse heating into the liquid state assumed a constant emissivity value in the liquid phase equal to the value deduced from the melting transition [7, 8]. In the following section, we describe the construction and operating principles of a laser polarimeter (DOAP) system that makes direct measurements of the optical constants n and k, from which the normal spectral emissivity can be derived in the liquid state during rapid pulse-heating experiments.

2.2. Normal Spectral Emissivity

Figure 1 shows the setup of the μs-DOAP system. As a result of the rapid changes in the current through the sample that occur during a pulse-heating experiment, both the source of light and the electronics are placed in a shielded room. The signals from the experiment are transferred by means of optical waveguides into the shielded room. A semiconductor laser diode, which produces radiation at a wavelength of 684.5 nm, serves as the light source. This light is amplitude modulated at a frequency of 8 MHz.

The light from the optical waveguide is delivered to the polarization state generator (PSG), which consists of a pair of motorized rotators that hold a linear polarizer and a quarter wave retarder which can generate any desired incident polarization state and deliver it to the specimen. The polarized and modulated laser beam is focused onto the sample, and the reflected light is collected by the polarization state detector (PSD). The PSD divides the reflected laser beam into four beams, which are collected by optical waveguides and delivered to four Si photodiodes. The detector output is demodulated using a lock-in technique with an output bandwidth approaching 1 MHz. From the four obtained signals, $\mathbf{I} = (I_0, I_1, I_2, I_3)$, one obtains via the inverse instrument matrix $\mathbf{F^{-1}}$ the four components of the Stokes vector $\mathbf{S} = (S_0, S_1, S_2, S_3)$ of the reflected laser beam, from which the specimen properties can be derived.

$$\vec{S} = F^{-1}\vec{I} \tag{4}$$

The matrix $\mathbf{F}$ is determined separately from a calibration procedure [9]. If the incident polarization state is set $+45°$ (linear), and the reflected Stokes
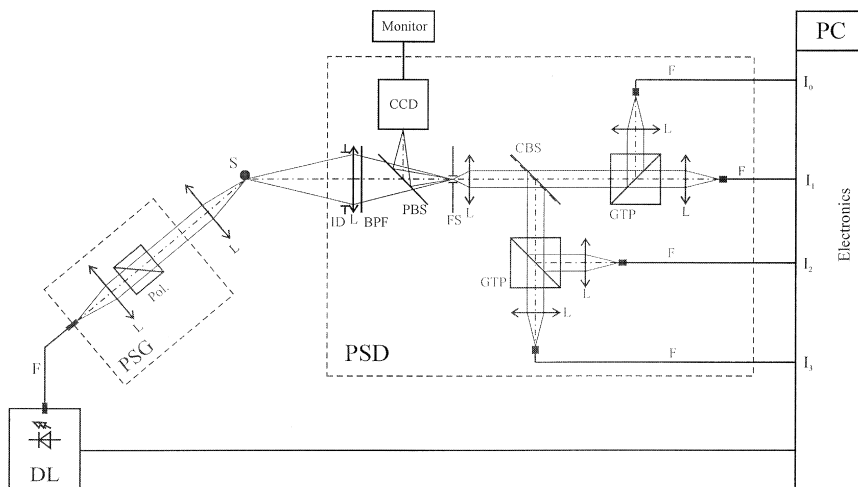
Fig. 1. Schematic of the μs-DOAP. CCD, CCD camera with monitor; PSG polarization state generator; PSD, polarization state detector; DL, diode laser; Pol., polarizer; L, lenses; S, sample; BPF, band pass filter; PBS, pellicle beam splitter; CBS, coated beam splitter; GTP, Glan–Thomson prism; F, fiber; ID, iris diaphragm; FS, field stop; I_0, I_1, I_2 and I_3, four intensities pictured to diodes; PC, personal computer.

parameters (S_0, S_1, S_2, S_3) are measured, the ellipsometric parameters, ψ and Δ, are given by

$$\psi = \frac{1}{2} \tan^{-1} \left[\frac{\sqrt{S_3^2 + S_2^2}}{-S_1} \right] \tag{5}$$

$$\Delta = \tan^{-1} \left[\frac{-S_3}{S_2} \right] \tag{6}$$

The values of ψ, Δ, and the incidence angle Θ yield the refractive index n and the extinction coefficient k of the reflecting material using the following equation:

$$n - ik = n_0 \tan(\Theta) \left[1 - \frac{4\rho \sin^2(\Theta)}{(1+\rho)^2} \right]^{\frac{1}{2}} \tag{7}$$

where $\rho = \tan(\psi) \exp(i\Delta)$ and n_0 is the refractive index of the transparent ambient medium.

Once n and k have been determined, the normal spectral reflectivity R_λ is calculated from the following equation:

$$R_\lambda = \frac{(n - n_0)^2 + k^2}{(n + n_0)^2 + k^2} \tag{8}$$

For opaque materials the normal spectral emissivity ε_λ is then determined from Kirchoff's law:

$$\varepsilon_\lambda = 1 - R_\lambda \tag{9}$$

3. RESULTS

Figure 2 presents the time-dependent behavior of the four intensity signals obtained by the DOAP system and the corresponding radiance temperature of a single experiment on niobium. All four DOAP signals have a strong rise in intensity at the start of melting. This can be explained by the reduction in surface roughness and the formation of a specular liquid surface, giving rise to an increase in reflectivity.

For both the solid and the liquid states, the noise of the demodulated signals should have the same value, but it is observed that the signals in the liquid state are associated with substantially greater noise. This noise appears to be correlated among the four channels and might be associated with

the non-Gaussian shape of the laser beam or with fast oscillations of the sample surface. As stated previously, the laser light source is delivered to the specimen using an optical fiber. Due to the small surface of the wire ($\varnothing$, 0.5 mm), only a small amount of intensity is reflected; therefore, a multimode fiber is used. To get more reflected intensity, the laser beam is focused onto the sample surface. Multimode fibers are always associated with a strong non-Gaussian profile (see Fig. 5). This arrangement is very sensitive to specimen motion. Since the sample expands significantly during the experiment, especially in the liquid state, it is believed that this correlated noise arises due to reflection by the wire from different points of varying intensity across the multimode laser beam profile.

Figure 3 depicts normal spectral emissivity at 684.5 nm versus time for the same experiment. The start of the experiment at room temperature is at 0 μs, the polarimeter signals and thus the calculated emissivity values are strongly disturbed by the firing of the ignitron, which is used as a fast current switch. The liquid phase begins at about 25 μs and ends at about 35 μs. Three peaks can be observed in this time interval which match exactly with the correlated noise peaks discussed previously (Fig. 2). A strong peak at 34 μs corresponds to the collapse of four signals (see Fig. 2). The behavior of the emissivity in the solid state is quite noisy, but the emissivity in the solid is not very repeatable since emissivity is influenced mainly by the roughness of the surface. To obtain reproducible values for the solid state,
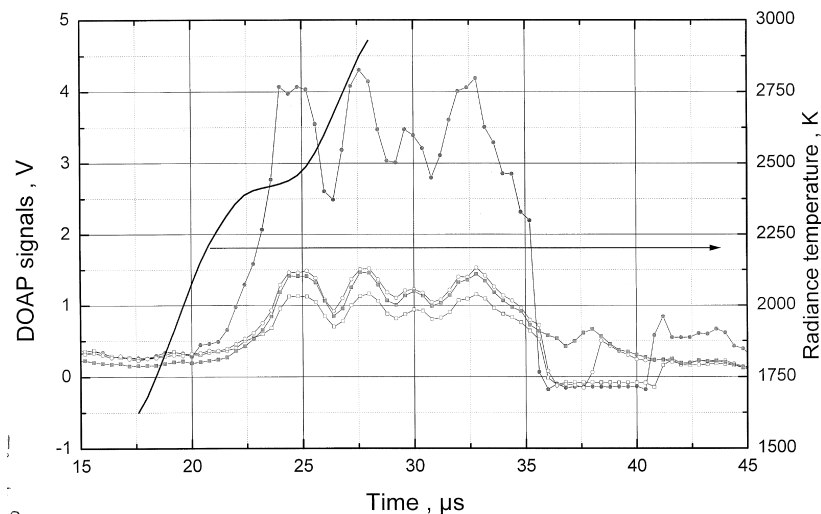

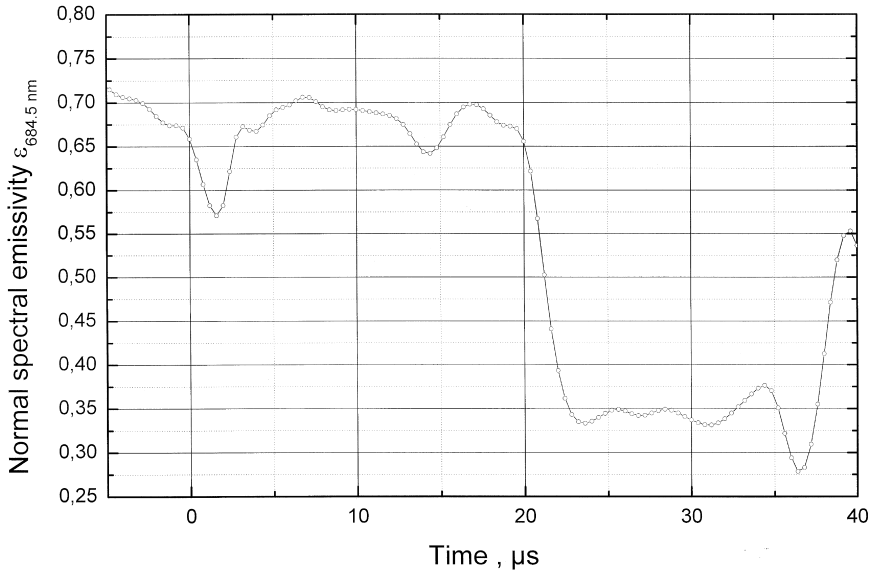**Fig. 2.** Four intensity signals of the DOAP as well as radiance temperature versus time for an experiment on niobium.

Fig. 3. Emissivity at 684.5 nm for a single experiment on a niobium sample versus time.
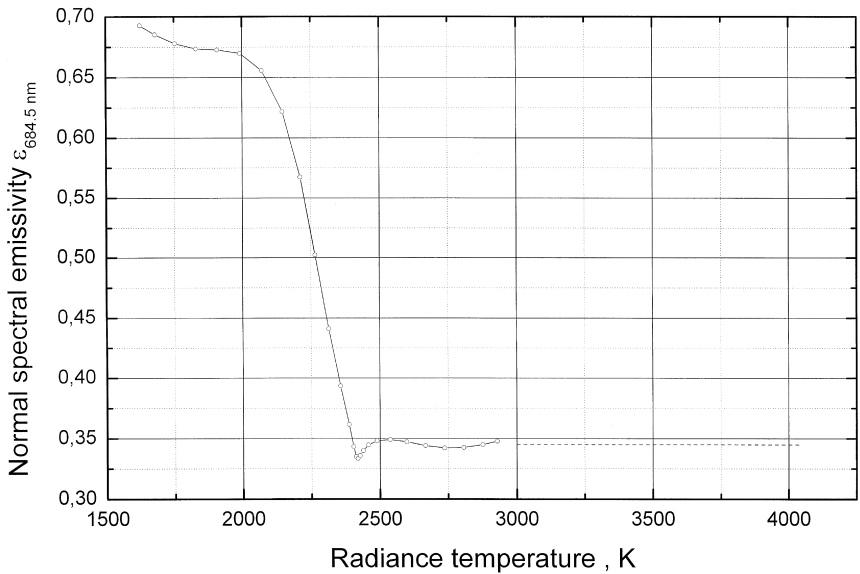

Fig. 4. Emissivity at 684.5 nm as function of radiance temperature for niobium. The solid line indicates measured values up to 3000 K, and the dashed line shows an extrapolation up to 4000 K.

one must preheat the sample several times close to melting to smooth the surface and to eliminate contaminants [10, 11].

The dependence of normal spectral emissivity at 684.5 nm on radiance temperature is presented in Fig. 4. Since the amplifier of our pyrometer has an upper radiance temperature limit of about 3000 K, measured values are available only up to this temperature. To obtain values at higher temperatures, one would have to decrease the radiance from the sample using neutral density filters or by varying the amplification.

In Fig. 4 the spectral emissivity drops in the solid phase from a value of 0.7 at room temperature to a value of 0.33 at the onset of melting. At the end of melting the emissivity increases slightly to 0.345 and remains more or less constant up to 3000 K (radiance temperature).

4. DISCUSSION

If we assume a linear increase in temperature with time, we obtain a radiance temperature of 4000 ± 50 K at the point of the collapse of the four intensity signals at 30 μs. With an emissivity value of 0.345 measured by the DOAP, we obtain a true temperature of 5000 ± 70 K. This value is in reasonable agreement with the boiling point of niobium (5017 K according to Ref. 12). This would indicate that the DOAP system might provide emissivity values for the whole liquid state for niobium.

The beam shape of the laser, after the optical waveguide and the PSG module, is shown in Fig. 5. One can see that individual fibers of the waveguide show different polarization states. Depending on the polarization state of the corresponding fiber, one receives, after the linear polarizer and the quarter wave retarder of the PSG module, a corresponding intensity, which leads to the shown beam shape. To avoid this problem, we plan to eliminate the waveguide and to position the laser in a shielded box in front of the PSG module to obtain a perfect gaussian beam profile and thus avoid the strong variations of intensity in the liquid phase.

The absolute accuracy of the DOAP measurements of normal spectral emissivity is estimated to be ± 0.015 or about $\pm 5\%$ for the present measurements. This uncertainty is greater than that which would be predicted from the polarization state measuring ability of the instrument but consistent with the known properties of niobium at the melting point [13]. Independent measurements on reference surfaces showed that the index of refraction, n, on a BK7 glass surface was measured to an uncertainty of 0.5% or better (as this is an average of about 1000 data points). The precision of the measurements is also somewhat larger, approximately, ± 0.01, due to the fact that measurements on the liquid state are considerably more
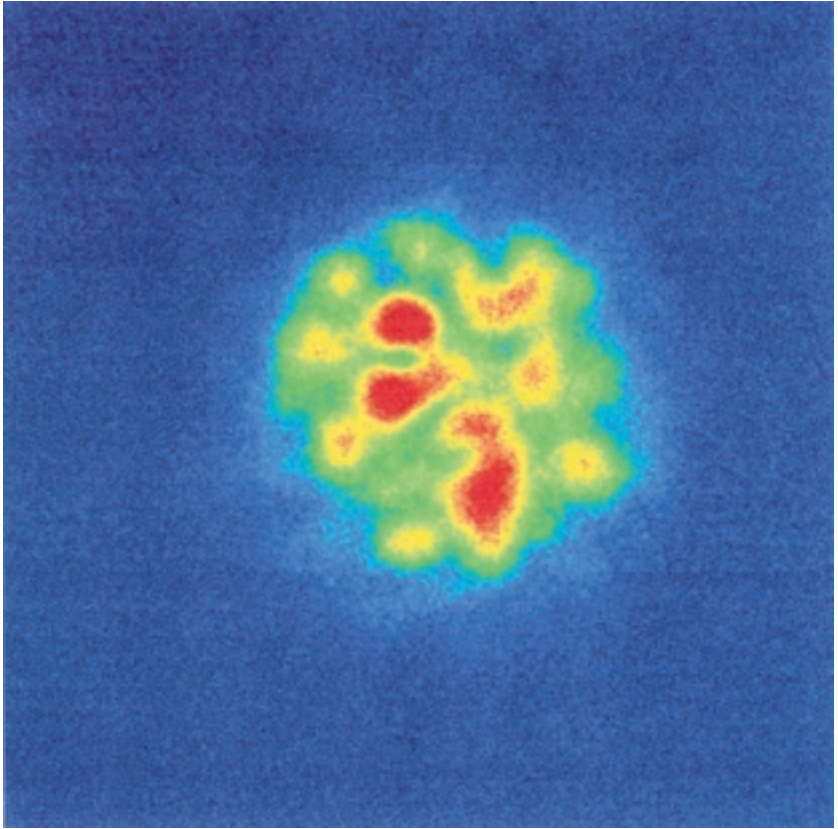
Fig. 5.   Beam profile of the laser beam after the PSG module, detected by a 12-bit intensified CCD camera.

difficult because of the speed, high background radiance, and rapid change in intensity which occur due to the non-Gaussian beam profile. Further details on temperature evaluation uncertainties have been discussed in Section 2.1.

5. CONCLUSION

In this work the first emissivity values at 684.5 nm of liquid niobium up to 3500 K were obtained experimentally.

ACKNOWLEDGMENTS

REFERENCES

1. G. Pottlacher, T. Neger, and H. Jäger, *Int. J. Thermophys.* **7**:149 (1986).
2. A. Seifter, G. Pottlacher, H. Jäger, G. Groboth, and E. Kaschnitz, *Berichte Bunsengesellschaft* **102**:1266 (1998).
3. G. Pottlacher, *J. Non-Crystall. Solids* **250–252**:177 (1999).
4. A. Cezairliyan, M. S. Morse, H. A. Berman, and C. W. Beckett, *J. Res. NBS* **74A**:65 (1970).
5. A. Cezairliyan and F. Righini, *Metrologia* **33**:299 (1996).
6. R. M. A. Azzam, *Opt. Acta* **29**:685 (1982).
7. G. R. Gathers, *Int. J. Thermophys.* **4**:149 (1983).
8. G. Pottlacher and H. Jäger, in *Proc. TEMPMEKO 96*, P. Macarino, ed. (Levrotto & Bella, Torino, 1997), p. 493.
9. S. Krishnan, *J. Opt. Soc. Am.* **9**:1615 (1992).
10. K. Boboridis, *Int. J. Thermophys.* (in press).
11. E. C. Horrigan, J. Haidar, and F. Righini, *Int. J. Thermophys.* **17**:1037 (1996).
12. D. R. Lide, *CRC Handbook of Chemistry and Physics* (CRC Press, New York, 1997).
13. A. Cezairliyan and A. P. Miller, *Int. J. Thermophys.* **13**:39 (1992).